ACS APPLIED MATERIALS & INTERFACES

Research Article

www.acsami.org

Programmable Macroscopic Supramolecular Assembly through Combined Molecular Recognition and Magnetic Field-Assisted Localization

Mengjiao Cheng, Qian Liu, Yiming Xian, and Feng Shi*

State Key Laboratory of Chemical Resource Engineering & Key Laboratory of Carbon Fiber and Functional Polymer, Ministry of Education, Beijing University of Chemical Technology, 15 Beisanhuan East Road, Chaoyang Distrist, Beijing 100029, China

Supporting Information

ABSTRACT: Macroscopic supramolecular assembly is a promising bottom-up method to construct ordered three-dimensional structures in a programmable way because of its flexible tailoring features. To handle the challenges of precisely aligning the building blocks, we proposed the combination of magnetic field-assisted localization for the locomotion of building blocks and host/guest supramolecular recognition for their immobilization. By applying this strategy, we have realized the stepwise construction of microscale glass fibers into an ordered complex pattern. Furthermore, through the introduction of a competitive guest molecule to disassemble the assembled structure, we demonstrated that the interaction between the fibers and the substrate was supramolecular rather than nonselective stickiness. Multivalent theory was used to interpret the mechanism for the interaction process.

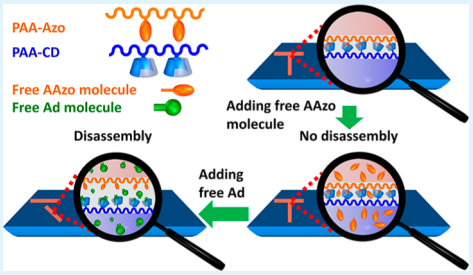

KEYWORDS: *macroscopic supramolecular assembly, ordered three-dimensional structure, magnetic field-assisted localization, multivalency*

INTRODUCTION

The construction of ordered three-dimensional (3D) structures can enhance the mechanical properties of reinforcing hybrid materials[1,2] and create periodicity in optical crystals,[3,4] as well as provide desired 3D scaffolds for tissue engineering.[5] Currently, few methods have been proposed for the fabrication of 3D ordered structures with building blocks having a feature size of 10 μm to millimeters; these methods include microelectromechanical systems,[3] 3D printing,[6] two-photon polymerization,[7,8] and self-assembly.[9−11] Among these, macroscopic supramolecular assembly as a bottom-up method is advantageous because the assembly process can be tailored and the species are biocompatible for applications in tissue engineering.[12,13] However, the fabrication of 3D ordered structures through supramolecular assembly is challenging because aligning the building blocks in well-defined geometries is difficult. To overcome this challenge, building blocks can be fabricated with specific shapes and sizes; additionally, selective surface modification can be used to introduce anisotropic chemical properties to the assembling components, which may lead to assemblies of complementary shapes or aggregates through molecular recognition of surface groups. Whitesides et al. demonstrated ordered two-dimensional (2D) assemblies with energetically favorable structures formed by millimeter epoxy or polydimethylsiloxane building blocks via shape-selective lock-and-key geometry control under oscillation to break nonselective aggregates.[14] Similarly, Xu et al. reported direct self-assembly of microscale positive and negative hydrogels of complementary shapes using electrostatic interactions as the binding force.[15] By using selective surface modification, Whitesides et al. introduced different wettabilities of the building block surfaces, which showed different menisci at the water−oil interface and led to an ordered array of millimeter-scale objects because of minimization of the interfacial free energy of the liquid−liquid interface.[16] Yin et al. decorated prescribed surfaces of a cubic hydrogel building block using DNA glue to create an asymmetric surface modification of interactive groups; the hydrogels with complementary DNA strands on specific surfaces could form complex assemblies in a programmed manner.[17] Although shape-selective or face-specific building blocks can form desired ordered structures through random locomotion and collision of the building blocks, such building blocks are too complex to fabricate, especially with microscale feature sizes. Therefore, developing a versatile method is important to control the locomotion of building blocks for specific assembly through surface interactive groups.

Although various strategies have been used to control the locomotion of macroscopic objects, including oxygen bubble propulsion by decomposition of hydrogen peroxide,[18−22] hydrogen bubble propulsion through the reduction of protons by zinc,[23] locomotion driven by Maragoni effects,[24] and

Received: February 12, 2014
Accepted: April 9, 2014
Published: April 9, 2014

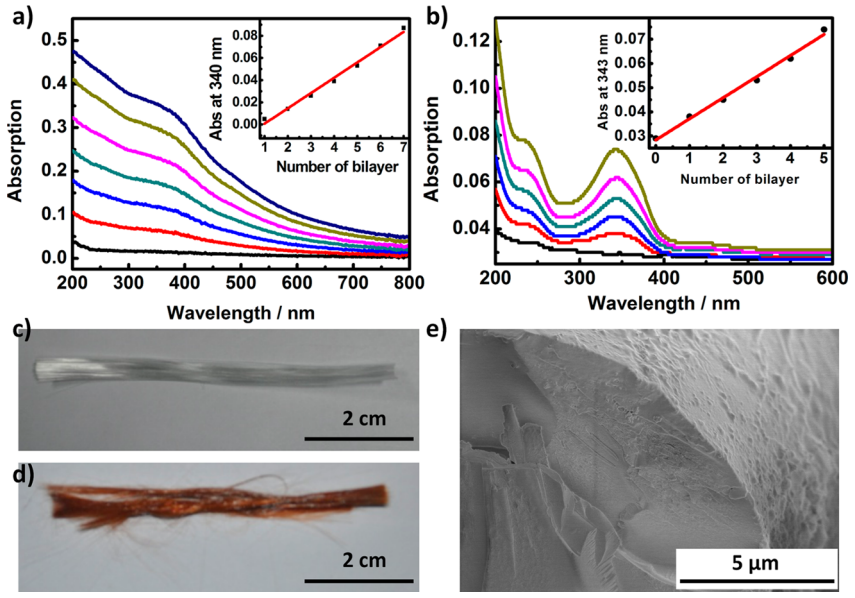

Figure 1. UV−visible spectra of the (a) PAA/Fe_3O_4 MNPs multilayer and (b) PDDA/PAA−Azo multilayer measured after each bilayer deposition; the insets show the linear correlations between the absorbance at a specific wavelength and the number of deposited bilayers. The appearance of the glass fibers (c) before and (d) after surface modification of PAA/Fe_3O_4 MNPs bilayers. (e) The SEM image of a (PAA/Fe_3O_4 MNPs)$_{20}$−(PDDA/PAA−Azo)$_{20}$ multilayer.

biomotors,[25] applying a magnetic field showed remarkable advantages in guiding the building blocks to locomote in a controlled way during assembly. This is because a magnetic field can be applied to objects of a wide size range, from the nano- to macroscale, using a noncontact method.[26−31] Additionally, the magnetic field approach is effective, environmentally benign, and provides chemical-free control of the systems. We have previously driven a glass fiber modified with multilayers containing Fe_3O_4 magnetic nanoparticles (MNPs) on the surface of water in the presence of an external magnetic field and evaluated the average force load of each MNP.[30,32] Similarly, Whitesides et al. coembedded magnetic and nonmagnetic nanowires to deliver the nonmagnetic nanowire by magnetic force.[33] We applied a magnetic field to transport a fiber to the desired location and immobilize it onto a substrate by coordination bonding between the fiber and the substrate, leading to an ordered complex pattern.[32] However, two challenges still remain in the magnetic-assisted supramolecular assembly at the macroscopic scale: one is to eliminate the human intervention of pressing the fiber through a needle to force it to reach the interactive distance of coordination, which could be handled by increasing the interaction between the fiber and the substrate; the other is to realize the disassembly process of the magnetic-assisted supramolecular assembly, which could be achieved by introducing competitive guest molecules. Herein, we report strong host/guest supramolecular recognition of cyclodextran (CD)/azobenzene (Azo) groups to immobilize magnetically responsive glass fibers onto the substrate, assisted by the localization of a magnetic field. Because of the stronger interaction between microscale building blocks compared to the coordinating binding in our previous results,[32] the surface host or guest groups could reach within the interactive distance when complementary assembling components approached. Thus, this approach avoids the need for mechanical pressing and results in self-assembly of a regular and ordered complex pattern. Moreover, the assembling mechanism between the glass fibers and the substrate has been further explored and demonstrated by the theory of multivalency in the current work. To confirm this hypothesis, we have introduced a competitive guest molecule, an adamantine (Ad) group, and the assembled structure could be disassembled because of the competitive host/guest molecular recognition and displacement of the Azo group. The results proved that the interaction between the fibers and the substrate was supramolecular rather than nonselective stickiness, indicating that the assembling mechanism was multivalent interaction. The current work not only demonstrates a facile way to construct ordered complex structures through supramolecular assembly but also provides a better understanding for the supramolecular interactive process.

RESULTS AND DISCUSSION

Introducing Magnetic Responsive Film and Host/Guest Groups. In this study, we used quartz glass fiber with a diameter of 17 μm and an average length of 1 mm as the building block and a quartz glass slide (1 cm × 3 cm) as the substrate. To induce magnetic responsive properties in the glass fibers for magnetically controlled movement and to introduce supramolecular guest groups on the outer surface, we first modified the glass fibers using a layer-by-layer (LbL) self-assembly technique, which is a versatile and controllable method used to construct multilayer ultrathin films. The glass fibers were modified in the following sequence. The glass fibers were modified with MNPs by using a similar LbL procedure described in our previous work.[32] The glass fibers were deposited with one bilayer of poly(diallyldimethylammonium chloride) (PDDA, aq, 1 mg mL^{-1})/poly(acrylic acid) (PAA, aq, 1 mg mL^{-1}). Next, the glass fibers were alternately immersed in an ethanol solution of PAA (1 mg mL^{-1}) and a hexane solution of Fe_3O_4 MNPs for 20 min each, leading to a multilayer of PAA/MNPs. In this way, the magnetically responsive MNPs could be incorporated into the polyelectrolyte multilayer on the surface of the glass fibers, which could be driven in the presence of a magnetic field. The stepwise LbL process was monitored

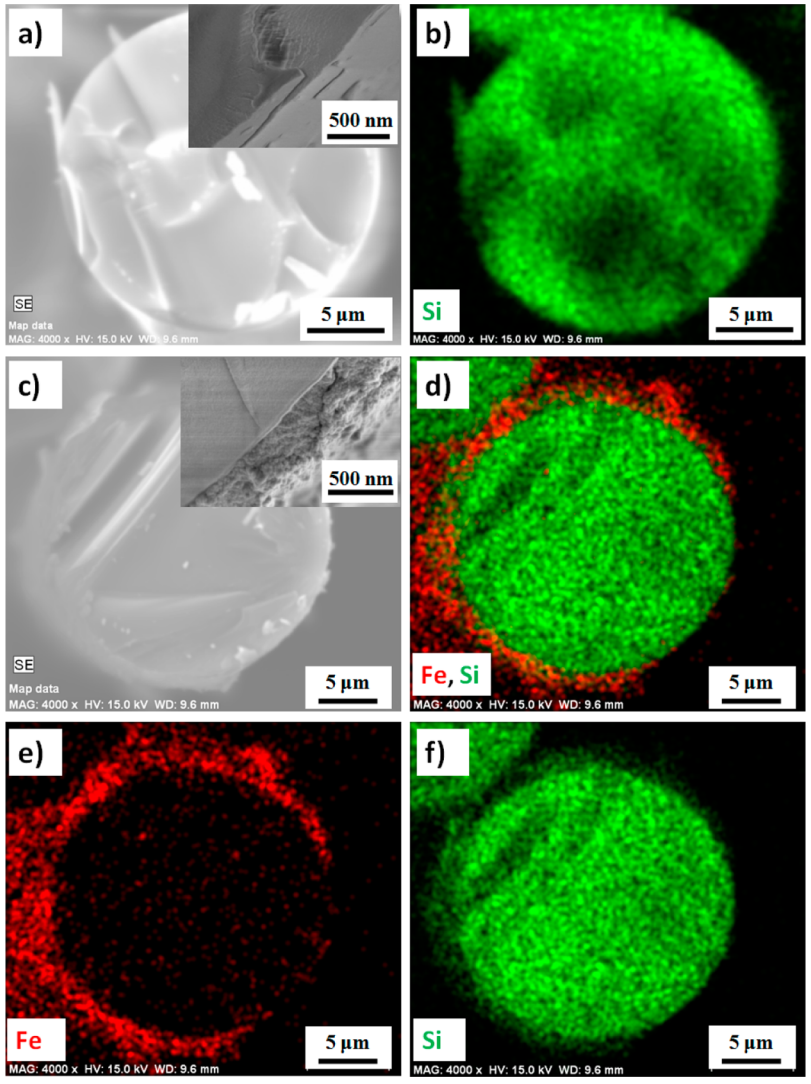

Figure 2. SEM images of (a) bare glass fibers and (c) glass fibers with $(PAA/Fe_3O_4\ MNPs)_{20}$ multilayers. EDX mapping patterns of (b) Si corresponding to a and (d–f) Si–Fe overlapped patterns, single Fe pattern, and single Si pattern corresponding to c, respectively.

using ultraviolet–visible spectroscopy as each Fe_3O_4 MNP layer was deposited. Figure 1a shows a broad absorption peak in the range from 300 to 400 nm, which is attributable to the ligand field transition and charge-transfer transition of the Fe_3O_4 MNPs.[34] We could detect the relative amount of Fe_3O_4 MNPs absorbed on the quartz substrate by monitoring the absorbance spectra as each PAA/Fe_3O_4 bilayer was deposited; the absorbance increased by a constant amount with each bilayer. Additionally, each deposition of Fe_3O_4 MNPs was linearly correlated with the number of bilayers by tracing the absorbance values at 340 nm, as shown in the inset of Figure 1a. The amount of absorbed Fe_3O_4 MNPs within each bilayer was nearly constant and could be controlled by the number of deposition cycles.

Similarly, the surface host or guest groups were also introduced by LbL assembly above the PAA/MNPs bilayer. First, we grafted the host (CD) or guest (Azo) functional groups bearing amino groups onto the PAA chain to obtain PAA–CD or PAA–Azo, respectively (experimental details are provided in the Supporting Information). Then, PAA–CD (aq, 1 mg mL^{-1}) or PAA–Azo (aq, 1 mg mL^{-1}) was combined with PDDA (aq, 1 mg mL^{-1}) via LbL assembly to generate a multilayer of PDDA/PAA–CD or PDDA/PAA–Azo on the quartz substrate or glass fibers, respectively. The LbL process for PDDA/PAA–Azo is discussed as an example. The strong peak at 345 nm accompanied by absorption at 240 nm indicates the presence of PAA–Azo (Figure 1b); the amount of PAA–Azo increased linearly with the number of PDDA/PAA–Azo bilayers, as shown in the inset of Figure 1b. The appearance of the glass fibers changed from colorless (Figure 1c) to brown (Figure 1d) after modification with the PAA/Fe_3O_4 MNPs bilayer; this color change was due to the brown color of the MNP dispersion. The glass fibers showed almost no color change after PDDA/PAA–Azo deposition. The surface morphology of the $(PAA/Fe_3O_4\ MNPs)_{20}$–$(PDDA/PAA–Azo)_{20}$ multilayer was characterized with scanning electron microscopy (SEM). Figure 1e shows that after PDDA/PAA–Azo deposition, the glass fiber was entirely wrapped in a homogeneous film with slightly protruding islands. Considering the rough PAA/Fe_3O_4 MNPs multilayer and high curvature of the glass fiber, we further characterized the surface morphology of the $(PDDA/PAA–Azo)_{20}$ multilayer alone on a quartz plate using atomic force microscopy (see Figure S5 in the Supporting Information). The height image reveals that the film surface

was slightly wrinkled with nanoscale pores; the corresponding phase image indicates that the film was homogeneous with small islands.

To further confirm the composition of the assembled composites, we used SEM cross-sectional images and the corresponding elemental mapping patterns from energy-dispersive X-ray spectroscopy (EDX) to characterize the glass fibers. As shown in Figure 2a, the cleaned and cut glass fibers had an average diameter of 17 μm and a rough cross-sectional surface due to the fracturing procedure. The mapping pattern of a single glass fiber (Figure 2b) shows that silicon was dispersed throughout the cross-section of the glass fiber and on part of an adjacent fiber, confirming a dominant presence of SiO_2 from the bulk quartz glass fiber material. After surface modification with 20 bilayers of PAA/Fe_3O_4 MNPs, the glass fiber was surrounded by a thin layer of film (Figure 2c); magnification of the glass fiber showed that the film was composed of closely packed nanoparticles along the edge of the fiber, exhibiting a film thickness of around 300 nm. Because the number of layers was known to be 20, we could calculate the average thickness of one PAA/Fe_3O_4 MNPs bilayer as 15 nm, which corresponded well with the diameter of the Fe_3O_4 MNPs (15−20 nm based on transmission electron microscopy images; see the Supporting Information). Moreover, the overlaid elemental mapping patterns of Fe and Si (Figure 2d) showed that Si was dominant in the cross-sectional region of the fiber, whereas Fe was dominant around the cross-section; this is attributable to Fe within the PAA/Fe_3O_4 MNPs bilayers on the cylindrical surface of the glass fiber. Separate elemental mapping images (Figure 2e, f) showed that Fe was also randomly distributed in the glass fiber cross-sectional surface, which may have resulted from fragmentation of PAA/Fe_3O_4 MNPs bilayers during the fracturing process. Such fragments were randomly distributed on the cross-sectional surface of the fiber shown in Figure 2c. These results demonstrated that Fe_3O_4 MNPs were successfully loaded onto the surface of the glass fiber, which was expected to exhibit magnetically responsive properties.

Magnetic Field-Assisted Localization of Microscale Glass Fibers and Their Immobilization for Programmable Supramolecular Assembly. We applied an external magnetic field by placing a magnet above a Petri dish containing the glass fiber modified with (PAA/Fe_3O_4 MNPs)$_{20}$−(PDDA/PAA−Azo)$_{20}$ multilayers in water. As expected, the glass fiber rapidly responded to the magnetic field, and the locomotion of the fiber was controlled by moving the magnet. The number of bilayers of PAA/Fe_3O_4 MNPs on the glass fiber was determined by the responsiveness to the magnetic field, which was dependent on the amount of Fe_3O_4 MNPs. Therefore, to determine the optimum number of bilayers, we identified the minimum number of bilayers that enabled sufficient magnetic control over the locomotion of the glass fibers. We adjusted the number of PAA/Fe_3O_4 MNPs bilayers on the glass fibers from 5 to 10, 15, and 20, while keeping all other conditions constant, and checked the magnetic responsiveness of the as-prepared fiber in water. The results showed that 5 or 10 bilayers were not sufficient to move the glass fibers due to the relatively low amount of MNPs. Increasing the number of bilayers to 15 caused the fiber to move slightly, but the magnetic control of the movement was poor. When the number of bilayers exceeded 20, the glass fiber responded well and was controlled by the magnetic field. The movement of glass fibers is determined by the force balance of all the forces applied to the fibers: gravity, buoyancy, and magnetic lifting forces. Considering that the density of quartz (about 2.2−2.6 g cm^{-3}) is much higher than that of water, the magnetic lifting force should be larger than the difference between gravity and buoyancy within water. As the number of PAA/Fe_3O_4 MNPs bilayers increased, the amount of Fe_3O_4 MNPs increased and contributed to the enhanced magnetic force, which balanced the force of gravity.

To realize programmable macroscopic supramolecular assembly of glass fibers, we combined the magnetically responsive locomotion with supramolecular recognition between host groups of CD on the substrate and guest groups of Azo on the glass fiber. The following procedure was carried out, as illustrated in Scheme 1. First, a quartz slide modified with (PDDA/PAA−CD)$_{20}$ multilayers and an untreated quartz slide were placed side-by-side in a Petri dish containing water. The glass fiber with (PAA/Fe_3O_4 MNPs)$_{20}$−(PDDA/PAA−Azo)$_{20}$ multilayers was cut to an average length of 1 mm and dropped into the water onto the bare quartz slide. Because no interactive groups were present on the bare quartz substrate, the glass fiber could be picked up by a magnet and directed above the quartz slide containing the CD groups. Considering that all of the as-prepared glass fibers were responsive to magnetic field, we dropped few cut glass fibers that were scattered on the bare quartz substrate, applied the magnet above the desired glass fiber and rapidly moved it to a location far from other glass fibers. After the fiber was guided to the desired location, the magnet was quickly removed and the fiber dropped onto the substrate, leading to contact between the fiber/slide and a supramolecular interaction of the surface host/guest groups. To verify the stability of the glass fiber on the quartz slide, we moved the magnet directly above the fiber and attempted to pick up the fiber; the attempt failed, indicating that the glass fiber was successfully immobilized and further application of the magnetic field had little effect on the assembled structure. The number of PDDA/PAA−Azo multi-

Scheme 1. Illustration of the Programmable Assembly of Glass Fibers in a Petri Dish Containing Water[a]

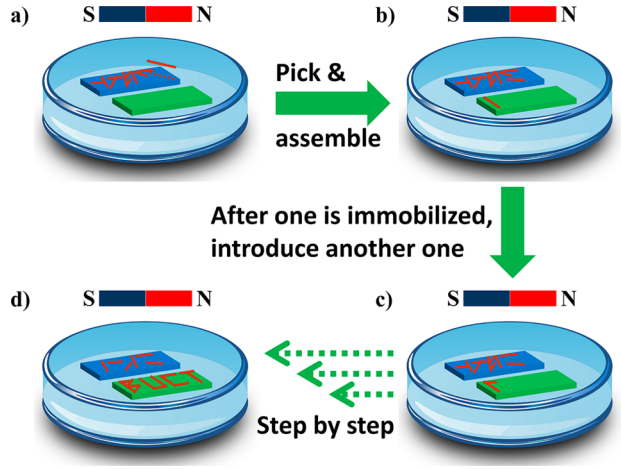

[a](a) Glass fibers with (PAA/Fe_3O_4 MNPs)$_{20}$−(PDDA/PAA−Azo)$_{20}$ multilayers were cut into 1 mm lengths and dropped onto a bare quartz substrate (blue); (b) one fiber was picked up and driven towards the adjacent quartz substrate (green) with the (PDDA/PAA−CD)$_{20}$ multilayer; (c, d) other fibers were transferred by magnetic field and assembled step-by-step, leading to a "BUCT" pattern.

dx.doi.org/10.1021/am500910y | ACS Appl. Mater. Interfaces 2014, 6, 7572−7578

layers was varied during immobilization. When the number of outer CD or Azo bilayers was 10 or 15, the glass fibers were not immobilized on the substrate, i.e., the fibers could be picked up by the magnetic field and removed from the substrate. When the number of CD or Azo bilayers reached 20 or 25, the fibers were successfully immobilized. Therefore, we determined that the optimum number of PDDA/PAA−CD or PDDA/PAA−Azo multilayers was 20. Finally, through step-by-step magnetic manipulation and immobilization of supramolecular interactions, we constructed an ordered complex pattern of "BUCT" using a programmable approach (Figure 3a). The accuracy of

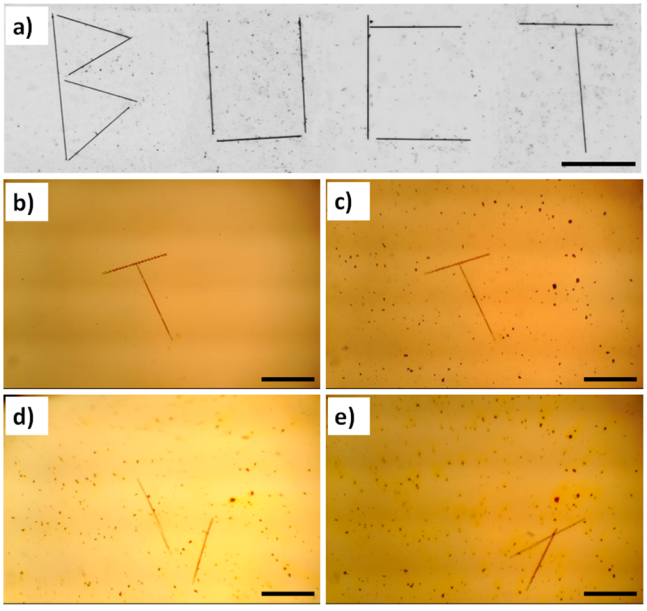

Figure 3. Optical microscopic photographs of (a) the assembled ordered complex pattern fabricated in a programmable way. The process of introducing free guest molecules: (b, c) the assembled 'T' pattern was stable after adding free 4-aminoazobenzene molecules, whereas (d, e) the structure completely disassembled after introducing competitive free 1-adamantanecarboxylic acid molecules. The scale bar is 500 μm.

the magnetically guided locomotion for assembly was evaluated by the reported method.[33] We evaluated the deviation of glass fibers perpendicular to each other ("UCT") in the assembled pattern, "BUCT". The perpendicular deviation from 90° over five pairs of glass fibers was 1.4 ± 1.5° and the center-to-center distance over five pairs of perpendicular glass fibers was 518 ± 42 μm. This method utilized a novel operating mode at the microscale, similar to a mini factory: the separate components (the as-prepared glass fibers) were stored in a warehouse (the bare quartz slide), necessary building blocks were driven by a magnetic field and delivered to a workshop (the quartz slide modified with CD groups), and the building blocks assembled into ordered structures or regular patterns according to the application. The construction process progressed in a programmable way and produced the desired "products" for specific applications.

Multivalency of the Supramolecular Assembly. Although the glass fibers could be assembled in a programmable manner using a quartz substrate, the assembly mechanism and nature of the interactions require further investigation. In contrast to our previous work, no mechanical pressing was required in the current study to immobilize the glass fibers onto the substrate, which was likely due to the strong binding constant between CD and Azo groups via a multivalent mechanism (Scheme 2).[35−37] In a typical multi-

Scheme 2. Schematic for the Assembly Mechanism of Glass Fibers on the Quartz Slide[a]

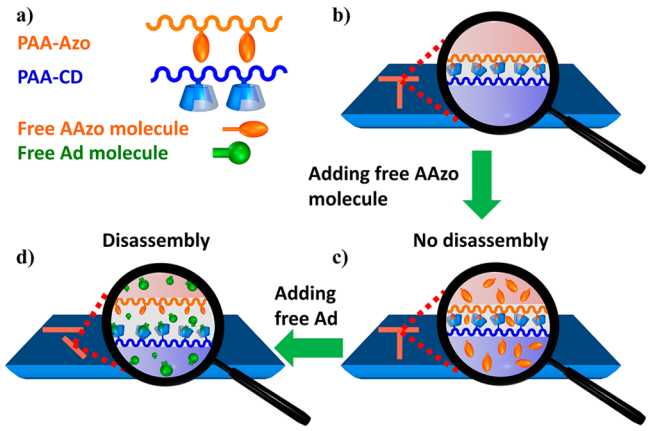

[a](a) Illustration of structures of grafted polyelectrolytes and free guest molecules; (b) the assembled glass fibers were attached to the substrate through CD−Azo interactions; (c) introducing free AAzo guest molecules did not lead to disassembly of the glass fiber pattern; (d) adding free Ad molecules resulted in disassembly of the glass fibers.

valent process, the local concentrations of CD and Azo groups increase as CD−Azo interactions occur, leading to more interactive CD−Azo pairs and enhancing the binding constant. In this process, the intrinsic binding constant of a single CD−Azo pair did not change, but the apparent association constant of multiple pairs of CD−Azo was significantly enhanced because of the increased probability of CD−Azo interactions facilitated by the high local concentrations of CD and Azo groups. According to multivalent theory, we assumed that the introduction of free guest molecules (e.g., 4-aminoazobenzene, AAzo) with binding constants similar to that of Azo−CD would not affect the assembled structure of CD−Azo interactions because the intrinsic binding constants between CD−Azo and CD−AAzo were almost identical. In contrast, adding highly competitive free guest molecules (e.g., 1-adamantanecarboxylic acid, Ad) might lead to disassembly of the fiber on the substrate because CD−Ad (1×10^5 M^{-1})[38,39] has a much higher intrinsic binding constant compared to CD−Azo (1×10^3 M^{-1}).[40] To confirm this hypothesis, we assembled a pattern of 'T' by combining the magnetic field-assisted locomotion of glass fibers with CD−Azo supramolecular interactions between the glass fibers and the substrate. Next, we added an aqueous AAzo solution at a low concentration (0.5 mM) to the assembled pattern and applied a magnetic field by placing the magnet above the 'T' pattern. As we moved the magnet over a narrow range to disturb the assembled 'T', the pattern remained unaffected (Figure 3b, c). Then silica nanoparticles were added to confirm the flow of the solution. The result confirmed that introducing guest molecules with similar binding constants had little effect on the assembled structure. Subsequently, we introduced the same amount of Ad solution (0.5 mM); within seconds, one glass fiber was removed from its original position (Figure 3d) followed by the displacement of the other glass fiber (Figure 3e; for the entire process, please see Movie S1 in the Supporting Information). The entire disassembly of the 'T'

dx.doi.org/10.1021/am500910y | ACS Appl. Mater. Interfaces 2014, 6, 7572−7578

pattern by highly competitive Ad molecules rather than AAzo molecules confirmed the hypothesis based on multivalent theory.

CONCLUSIONS

To summarize, we demonstrated the programmable macroscopic supramolecular assembly of glass fibers having an average diameter of 17 μm and average length of 1 mm by combining supramolecular recognition of CD−Azo and magnetic field-assisted manipulation. To enable the magnetic responsiveness of glass fibers in a magnetic field and supramolecular interactions, we used LbL assembly to modify the surface with a composite multilayer of $(PAA/Fe_3O_4$ MNPs$)_{20}$−$(PDDA/PAA−Azo)_{20}$, which rapidly responded to a magnetic field in a well-controlled way and effectively immobilized the fibers on the quartz substrate modified with $(PDDA/PAA−CD)_{20}$. The assembly mechanism of the glass fibers onto the quartz slide was interpreted based on multivalent theory, which was confirmed by introducing free guest molecules with highly competitive binding constants to disassemble the assembled pattern.

ASSOCIATED CONTENT

Supporting Information

Synthesis of PAA-CD and PAA-Azo, TEM images of Fe_3O_4 MNPs, AFM images of $(PDDA/PAA−Azo)_{20}$ multilayer, and Movie S1 of introducing competitive Ad for disassembly. This material is available free of charge via the Internet at http://pubs.acs.org.

AUTHOR INFORMATION

Corresponding Author

*E-mail: shi@mail.buct.edu.cn.

Notes

The authors declare no competing financial interest.

ACKNOWLEDGMENTS

This work was supported by NSFC (21374006), the Program of the Co-Construction with Beijing Municipal Commission of Education of China, Program for New Century Excellent Talents in University (NCET-10-0211), the Fok Ying Tung Education Foundation (131013), Open Project of State Key Laboratory of Supramolecular Structure and Materials (SKLSSM201401), and Beijing Young Talents Plan (YETP0488). We thank PPG Industries, Inc., for their generous providing glass fibers in all of the experiments.

REFERENCES

(1) Tang, Z. Y.; Kotov, N. A.; Magonov, S.; Ozturk, B. Nanostructured Artificial Nacre. *Nat. Mater.* **2003**, *2*, 413−418.

(2) Podsiadlo, P.; Kaushik, A. K.; Arruda, E. M.; Waas, A. M.; Shim, B. S.; Xu, J. D.; Nandivada, H.; Pumplin, B. G.; Lahann, J.; Ramamoorthy, A.; Kotov, N. A. Ultrastrong and Stiff Layered Polymer Nanocomposites. *Science* **2007**, *318*, 80−83.

(3) Lin, S. Y.; Fleming, J. G.; Hetherington, D. L.; Smith, B. K.; Biswas, R.; Ho, K. M.; Sigalas, M. M.; Zubrzycki, W.; Kurtz, S. R.; Bur, J. A Three-Dimensional Photonic Crystal Operating at Infrared Wavelengths. *Nature* **1998**, *394*, 251−253.

(4) Freymann, G. V.; Kitaev, V.; Lotsch, B. V.; Ozin, G. A. Bottom-up Assembly of Photonic Crystals. *Chem. Soc. Rev.* **2013**, *42*, 2528−2554.

(5) Ma, P. X. Scaffolds for tissue fabrication. *Mater. Today* **2004**, *7*, 30−40.

(6) Hutmacher, D. W. Scaffold Design and Fabrication Technologies for Engineering Tissues - State of the Art and Future Perspectives. *J. Biomater. Sci., Polym. Ed.* **2001**, *12*, 107−124.

(7) Wylie, R. G.; Ahsan, S.; Aizawa, Y.; Maxwell, K. L.; Morshead, C. M.; Shoichet, M. S. Spatially Controlled Simultaneous Patterning of Multiple Growth Factors in Three-Dimensional Hydrogels. *Nat. Mater.* **2011**, *10*, 799−806.

(8) DeForest, C. A.; Polizzotti, B. D.; Anseth, K. S. Sequential Click Reactions for Synthesizing and Patterning Three-Dimensional Cell Microenvironments. *Nat. Mater.* **2009**, *8*, 659−664.

(9) Gracias, D. H.; Tien, J.; Breen, T. L.; Hsu, C.; Whitesides, G. M. Forming Electrical Networks in Three Dimensions by Self-Assembly. *Science* **2000**, *289*, 1170−1172.

(10) Zhang, Z. K.; Pfleiderer, P.; Schofield, A. B.; Clasen, C.; Vermant, J. Synthesis and Directed Self-Assembly of Patterned Anisometric Polymeric Particles. *J. Am. Chem. Soc.* **2011**, *133*, 392−395.

(11) Wang, J. Y.; Wang, Y. P.; Sheiko, S. S.; Betts, D. E.; Desimone, J. M. Tuning Multiphase Amphiphilic Rods to Direct Self-Assembly. *J. Am. Chem. Soc.* **2012**, *134*, 5801−5806.

(12) Schulte, B.; Tsotsalas, M.; Becker, M.; Studer, A.; Cola, L. D. Dynamic Microcrystal Assembly by Nitroxide Exchange Reactions. *Angew. Chem., Int. Ed.* **2010**, *49*, 6881−6884.

(13) Harada, A.; Kobayashi, R.; Takashima, Y.; Hashidzume, A.; Yamaguchi, H. Macroscopic Self-Assembly through Molecular Recognition. *Nat. Chem.* **2011**, *3*, 34−37.

(14) Bowden, N.; Terfort, A.; Carbeck, J.; Whitesides, G. M. Self-assembly of Mesoscale Objects into Ordered Two-Dimensional Arrays. *Science* **1997**, *276*, 233−235.

(15) Han, Y. L.; Yang, Y. S.; Liu, S. B.; Wu, J. H.; Chen, Y. M.; Lu, T. J.; Xu, F. Directed Self-Assembly of Microscale Hydrogels by Electrostatic Interaction. *Biofabrication* **2013**, *5*, 035004.

(16) Bowden, N. B.; Weck, M.; Choi, I. S.; Whitesides, G. M. Molecule-Mimetic Chemistry and Mesoscale Self-Assembly. *Acc. Chem. Res.* **2001**, *34*, 231−238.

(17) Qi, H.; Ghodousi, M.; Du, Y.; Grun, C.; Bae, H.; Yin, P.; Khademhosseini, A. DNA-Directed Self-Assembly of Shape-Controlled Hydrogels. *Nat. Commun.* **2013**, *4*, 2275.

(18) Ismagilov, R. F.; Schwartz, A.; Bowden, N.; Whitesides, G. M. Autonomous Movement and Self-Assembly. *Angew. Chem., Int. Ed.* **2002**, *41*, 652−654.

(19) Kline, T. R.; Paxton, W. F.; Mallouk, T. E.; Sen, A. Catalytic Nanomotors: Remote-Controlled Autonomous Movement of Striped Metallic Nanorods. *Angew. Chem., Int. Ed.* **2005**, *44*, 744−746.

(20) Gao, Y. F.; Cheng, M. J.; Wang, B. L.; Feng, Z. G.; Shi, F. Diving-Surfacing Cycle within a Stimulus-Responsive Smart Device towards Developing Functionally Cooperating Systems. *Adv. Mater.* **2010**, *22*, 5125−5128.

(21) Ju, G. N.; Cheng, M. J.; Xiao, M.; Xu, J. M.; Pan, K.; Wang, X.; Zhang, Y. J.; Shi, F. Smart Transportation between Three Phases through a Stimulus-Responsive Functional Cooperating Device. *Adv. Mater.* **2013**, *25*, 2915−2919.

(22) Xiao, M.; Guo, X. P.; Cheng, M. J.; Ju, G. N.; Zhang, Y. J.; Shi, F. pH-Responsive On-Off Motion of a Superhydrophobic Boat: towards the Design of a Minirobot. *Small* **2013**, *10*, 859−865.

(23) Gao, W.; Uygun, A.; Wang, J. Hydrogen-Bubble-Propelled Zinc-Based Microrockets in Strongly Acidic Media. *J. Am. Chem. Soc.* **2012**, *134*, 897−900.

(24) Xiao, M.; Cheng, M. J.; Zhang, Y. J.; Shi, F. Combining the Marangoni Effect and the pH-Responsive Superhydrophobicity-Superhydrophilicity Transition to Biomimic the Locomotion Process of the Beetles of Genus Stenus. *Small* **2013**, *9*, 2509−2514.

(25) Schmidt, J. J.; Montemagno, C. D. Bionanomechanical Systems. *Annu. Rev. Mater. Res.* **2004**, *34*, 315−337.

(26) Liu, Y.-M.; Wang, W.; Zheng, W.-C.; Ju, X.-J.; Xie, R.; Zerrouki, D.; Deng, N.-N.; Chu, L.-Y. Hydrogel-Based Microactuators with Remote-Controlled Locomotion and Fast Pb^{2+}-Response for Micromanipulation. *ACS Appl. Mater. Interfaces* **2013**, *5*, 7219−7226.

(27) Torre, B.; Villafiorita-Monteleone, F.; Kostopoulou, A.; Nanni, G.; Falqui, A.; Casu, A.; Lappas, A.; Cingolani, R.; Athanassiou, A. Nanocomposite Pattern-Mediated Magnetic Interactions for Localized Deposition of Nanomaterials. *ACS Appl. Mater. Interfaces* **2013**, *5*, 7253−7257.
(28) Perineau, F.; Rosticher, C.; Rozes, L.; Chanéac, C.; Sanchez, C.; Constantin, D.; Dozov, I.; Davidson, P.; Rochas, C. Hybrid Nanocomposites with Tunable Alignment of the Magnetic Nanorod Filler. *ACS Appl. Mater. Interfaces* **2014**, *6*, 1583−1588.
(29) Yellen, B. B.; Friedman, G. Programmable Assembly of Colloidal Particles Using Magnetic Microwell Templates. *Langmuir* **2004**, *20*, 2553−2559.
(30) Shi, F.; Liu, S. H.; Gao, H. T.; Ding, N.; Dong, L. J.; Tremel, W.; Knoll, W. Magnetic-Field-Induced Locomotion of Glass Fibers on Water Surfaces: towards the Understanding of How Much Force One Magnetic Nanoparticle Can Deliver. *Adv. Mater.* **2009**, *21*, 1927−1930.
(31) Kriha, O.; Becker, M.; Lehmann, M.; Kriha, D.; Krieglstein, J.; Yosef, M.; Schlecht, S.; Wehrspohn, R. B.; Wendorff, J. H.; Greiner, A. Connection of Hippocampal Neurons by Magnetically Controlled Movement of Short Electrospun Polymer Fibers-A Route to Magnetic Micromanipulators. *Adv. Mater.* **2007**, *19*, 2483−2485.
(32) Cheng, M. J.; Gao, H. T.; Zhang, Y. J.; Tremel, W.; Chen, J.-F.; Shi, F.; Knoll, W. Combining Magnetic Field Induced Locomotion and Supramolecular Interaction to Micromanipulate Glass Fibers: toward Assembly of Complex Structures at Mesoscale. *Langmuir* **2011**, *27*, 6559−6564.
(33) Lipomi, D. J.; Ilievski, F.; Wiley, B. J.; Deotare, P. B.; Lončar, M.; Whitesides, G. M. Integrated Fabrication and Magnetic Positioning of Metallic and Polymeric Nanowires Embedded in Thin Epoxy Slabs. *ACS Nano* **2009**, *3*, 3315−3325.
(34) Hsia, C. H.; Chen, T. Y.; Son, D. H. Size-Dependent Ultrafast Magnetization Dynamics in Iron Oxide (Fe_3O_4) Nanocrystals. *Nano Lett.* **2008**, *8*, 571−576.
(35) Mulder, A.; Auletta, T.; Sartori, A.; Ciotto, S. D.; Casnati, A.; Ungaro, R.; Huskens, J.; Reinhoudt, D. N. Divalent Binding of a Bis(adamantyl)-Functionalized Calix[4]Arene to β-Cyclodextrin-Based Hosts: an Experimental and Theoretical Study on Multivalent Binding in Solution and at Self-Assembled Monolayers. *J. Am. Chem. Soc.* **2004**, *126*, 6627−6636.
(36) Huskens, J.; Mulder, A.; Auletta, T.; Nijhuis, C. A.; Ludden, M. J. W.; Reinhoudt, D. N. A Model for Describing the Thermodynamics of Multivalent Host-Guest Interactions at Interfaces. *J. Am. Chem. Soc.* **2004**, *126*, 6784−6797.
(37) Fasting, C.; Schalley, C. A.; Weber, M.; Seitz, O.; Hecht, S.; Koksch, B.; Dernedde, J.; Graf, C.; Knapp, E.-W.; Haag, R. Multivalency as a Chemical Organization and Action Principle. *Angew. Chem., Int. Ed.* **2012**, *51*, 10472−10498.
(38) Gu, L.-Q.; Braha, O.; Conlan, S.; Cheley, S.; Bayley, H. Stochastic Sensing of Organic Analytes by a Pore-Forming Protein Containing a Molecular Adapter. *Nature* **1999**, *398*, 686−690.
(39) Rekharsky, M. V.; Inoue, Y. Complexation Thermodynamics of Cyclodextrins. *Chem. Rev.* **1998**, *98*, 1875−1917.
(40) Liu, Y.; Zhao, Y.-L.; Chen, Y.; Guo, D.-S. Assembly Behavior of Inclusion Complexes of β-Cyclodextrin with 4-Hydroxyazobenzene and 4-Aminoazobenzene. *Org. Biomol. Chem.* **2005**, *3*, 584−591.